An Adaptive ANOVA-Based Data-Driven Stochastic Method for Elliptic PDE with Random Coefficients

Xin Hu[1], Guang Lin[2,*], Thomas Y. Hou[1], Pengchong Yan[1]

[1]Applied and Computational Mathematics, California Institute of Technology, Pasadena, CA 91125, USA

[2]Pacific Northwest National Laboratory, Richland, WA 99352, USA

January 11, 2012

Abstract

Generalized polynomial chaos (gPC) methods have been successfully applied to various stochastic problems in many physical and engineering fields. However, realistic representation of stochastic inputs associated with various sources of uncertainty often leads to high dimensional representations that are computationally prohibitive for classic gPC methods. Additionally in the classic gPC methods, the gPC bases are determined based on the probabilistic distribution of stochastic inputs. However, the stochastic outputs may not share the same probabilistic distribution as the stochastic inputs. Hence, the gPC bases may not be the optimal bases for such systems, which causes the slow convergence of gPC methods for such stochastic problems. Here we present a general framework that integrates the adaptive ANOVA decomposition technique and the data-driven stochastic method to alleviate both of the two limitations. To handle high-dimensional stochastic problems, we investigate the use of adaptive ANOVA decomposition in the stochastic space as an effective dimension-reduction technique for high-dimensional stochastic problems. Three different ANOVA adaptive criteria are discussed.

To improve the slow convergence of gPC methods, we use the data-driven stochastic method (DDSM) which was developed by Cheng-Hou-Yan in [5]. This method has an offline computation and an online computation. In the offline computation, optimal gPC bases are obtained by Karhunen-Loéve (K-L) expansion of the covariance matrix of stochastic outputs obtained by ANOVA-based sparse-grid PCM. In the online computation, a Galerkin-projection based gPC method with the optimal bases developed in the offline computation is employed, which greatly speeds up the convergence. Numerical examples are presented for one-, two-dimensional elliptic PDE with random coefficients, and a two-dimensional

*Corresponding author. *Email address:* Guang.Lin@pnnl.gov (Guang Lin)

Helmhotz equation in random media (Horn problem) to show the accuracy and efficiency of the developed adaptive ANOVA-based DDSM method.

Keywords: Analysis of variance, Karhunen-Loéve expansion, uncertainty quantification, high dimensions, sparse grids.

1 Introduction

There has been growing interest and significant progress over the past decades on modeling complex physical, and engineering systems with uncertainties. However, in the simulation of real physical randomly heterogeneous systems, a realistic representation of stochastic inputs associated with various sources of uncertainty often leads to high dimensional representations that are computationally prohibitive for many numerical methods, such as generalized polynomial chaos (gPC) methods [38] and probabilistic collocation method (PCM) [37]. In this paper, we present a general framework that combines the ANOVA decomposition technique with the recently developed data-driven stochastic method (DDSM) [5] to alleviate the curse of dimensionality and slow convergence issues of gPC methods. For stochastic problems with high stochastic dimensions, we employ the functional ANOVA (ANalysis-Of-VAriance) method [15, 2] as a dimension-reduction technique. The ANOVA decomposition was introduced by Fisher [8]. Later, Hoeffding in 1948 successfully apply ANOVA decomposition to study U-statistics [16]. This method is motivated by the observation that for many real physical systems, only a relatively small number of stochastic dimensions are important and will significantly impact the outputs of the stochastic systems. ANOVA has also been used for uncertainty quantification in [36] and was employed in gPC for solving high-dimensional stochastic PDE systems in [9, 24, 25, 4, 11, 39]. In [9] ANOVA was integrated with a multi-element PCM. In [24], an adaptive version of ANOVA is developed to automatically detect the important dimensions. In [39], adaptive ANOVA methods based on three different adaptive criteria were proposed and compared.

The ANOVA decomposition results in a set of low-dimensional sub-problems in stochastic space. A sparse-grid PCM is used to solve these low-dimensional sub-problems efficiently. The PCM was first introduced by Tatang and McRae [33]. Rrecently Xiu and Hesthaven [37] have used a Lagrange polynomial interpolation to construct high-order stochastic collocation methods. The properties of PCM were extensively studied in the past 10 years. In [26, 27, 1], the errors of integrating or interpolating functions with Sobolev regularity were analyzed for Smolyak constructions based on the one-dimensional nested Clenshaw-Curtis rules. In [27], the degree of exactness of the Smolyak quadrature using the Clenshaw-Curtis and Gaussian one-dimensional rules was investigated. In [37], the efficiency of the Clenshaw-Curtis-based sparse grid stochastic collocation was demonstrated by comparing it with other stochastic methods on an elliptic problem. In 2003, Gerstner and Griebel [12] introduced the dimension-adaptive tensor product quadrature method. In [10], sparse grid collocation schemes were applied to solve stochastic natural convection problems. In [21, 22, 18, 13], a multi-element PCM was employed to study the random roughness problem, stochastic compressible flow and plasma flow problems. In [14, 23], an adaptive hierarchical sparse grid collocation algorithm has been developed.

In the classic gPC methods, the gPC bases are determined based on the probabilistic distribution of stochastic inputs. DDSM is inspired by the fact that the stochastic outputs may not share the same probabilistic distribution as the stochastic inputs. Hence, the distribution used for sparse-grid PCM may not be the optimal distribution to represent the solutions of such systems, which causes the slow convergence of sparse-grid PCM for such stochastic problems. To overcome this difficulty, we use DDSM [5] to obtain a set of problem-dependent optimal gPC bases to greatly speed up the convergence. The number of gPC modes to achieve a specified accuracy used in the ANOVA-based DDSM is much smaller than the classic gPC method, which greatly reduces the computational cost. In this work, an ANOVA-based DDSM is developed, which can be considered as a stochastic extension of the Proper Orthogonal Decomposition (POD) methods [31, 35], the original DDSM of Cheng-Hou-Yan [5], and the Multiscale Finite Element methods [17]. DDSM has an offline computation and an online computation. In the offline computation, optimal gPC bases are obtained by Karhunen-Loéve (K-L) expansion of the covariance matrix of stochastic outputs obtained by ANOVA-based sparse-grid PCM. In the online computation, a Galerkin-projection based gPC method with optimal bases developed in the offline computation is employed, which accelerates the convergence rate considerably.

The remainder of the paper is organized in the following way; section 2 describes the standard ANOVA decomposition, section 3 presents the DDSM, Section 4 introduces the ANOVA-DDSM. Section 5 shows the results obtained using ANOVA-DDSM and section 6 summarizes the findings.

2 Sparse-Grid Based Probabilistic Collocation Method

The general procedure for the PCM approach is similar to MC simulations, with a difference in selecting the sampling points and corresponding weights. The procedure consists of three main steps:

1. Generate N_c collocation points in probability space of random parameters as independent random inputs based on a quadrature formula;
2. Solve a deterministic problem at each collocation point;
3. Estimate the solution statistics using the corresponding quadrature rule,

$$\langle u(\boldsymbol{x},t)\rangle = \int_\Gamma u(\boldsymbol{x},t,\xi)\rho(\xi)d\xi \tag{1}$$

$$\approx \sum_{k=1}^{N_c} v(\boldsymbol{x},t,\xi_k)w_k, \tag{2}$$

$$\sigma(u)(\boldsymbol{x},t) = \sqrt{\int_\Gamma (u(\boldsymbol{x},t,\xi)-\langle u\rangle)^2\rho(\xi)d\xi} \tag{3}$$

$$\approx \sqrt{\sum_{k=1}^{N_c} v^2(\boldsymbol{x},t,\xi_k)w_k - \langle v\rangle^2}, \tag{4}$$

where $\rho(\xi)$ is the probabilistic distribution function (PDF) of random variable ξ, N_c is the number of quadrature points, $\{\xi_k\}$ is the set of quadrature points and $\{w_k\}$ is the corresponding set of weights, which are the combination of quadrature weights in each random dimension. In the second step of the PCM approach, as for MC, any existing code can be used to solve deterministic flow-and-transport equations. Extensive reviews on the construction of quadrature formulas may be found in [6] and [7]. Below, we provide a brief review of two different methods for selecting collocation points.

In this work, we use the Smolyak formula [32] to construct the collocation point set, which is a linear combination of tensor product formulas, and the resulting point set has a significantly smaller number of points than the full tensor product set. Recently, researchers [37, 19, 20] have used Lagrange polynomial interpolation to construct high order stochastic collocation methods based on sparse grids using the Smolyak formula [32]. Such sparse grids do not depend as strongly on the dimensionality of the random space and as such are more suitable for applications with high-dimensional random inputs. Detailed description on how to build the collocation point set can be found in [37, 19, 20].

3 Data-Driven Stochastic Method

Consider the stochastic PDE

$$\mathcal{L}(\mathbf{x},\omega)u(\mathbf{x},\omega) = f(x) \tag{5}$$

where $\mathbf{x} \in D, \omega \in \Omega$ and $\mathcal{L}(\mathbf{x},\omega)$ is a stochastic differential operator. The stochastic ingredient resides in the differential operator $\mathcal{L}(\mathbf{x},\omega)$ while $f(x)$ is purely deterministic. The authors heuristically argue that the bases only depend on $\mathcal{L}(\mathbf{x},\omega)$. Generally speaking, the bases can be obtained by solving (5) for one particular $f(x)$ in offline part. Then this set of bases could be used to solve other problems with different complicated $f(x)$.

Inspired by multiscale finite element method [17] and proper orthogonal decomposition (POD) method [31, 35], Cheng-Hou-Yan proposed an new algorithm, called Data-Driven Stochastic Method [5]. The authors tried to build up gPC bases under which the stochastic solutions have a sparse decomposition based on Karnunen-Loève (K-L) expansion. For $u(\mathbf{x},\omega) \in L^2(D \times \Omega)$, its K-L expansion reads as follows

$$u(\mathbf{x},\omega) = \mathbb{E}[u] + \sum_{i=1}^{\infty} \sqrt{\lambda_i}\xi_i(\omega)\phi_i(\mathbf{x}), \tag{6}$$

where $\{\lambda_i\}$ and $\{\phi_i(\mathbf{x})\}$ are the eigenpairs of the covariance kernel $C(\mathbf{x},\mathbf{y})$, i.e.

$$\int_D C(\mathbf{x},\mathbf{y})\phi(\mathbf{y})d\mathbf{y} = \lambda\phi(\mathbf{x}), \tag{7}$$

and $\{\xi_i(\omega)\}$ are random variables defined as

$$\xi_i(\omega) = \frac{1}{\sqrt{\lambda_i}}\int_D (u(\mathbf{x},\omega) - \mathbb{E}[u])\phi_i(\mathbf{x})d\mathbf{x}. \tag{8}$$

Moreover, these mutually uncorrelated random variables $\{\xi_i(\omega)\}$ satisfy

$$\mathbb{E}[\xi_i] = 0, \quad \mathbb{E}[\xi_i \xi_j] = \delta_{ij} \tag{9}$$

In numerical practice, only a finite series expansion is adopted, depending on the decay rate of the eigenvalues,

$$u(\mathbf{x}, \omega) = \mathbb{E}[u] + \sum_{i=1}^{N} \sqrt{\lambda_i} \xi_i(\omega) \phi_i(\mathbf{x}). \tag{10}$$

For a given covariance function, the decay rate of the eigenvalues depends inversely on the correlation length. Long correlation length implies that the random process is strongly correlated and results in a fast decay of the eigenvalues. A weakly correlated process has short correlation length and results in a slow decay of the eigenvalues. Under some assumptions [30], the eigenvalues in K-L expansion decay exponentially (or sub-exponentially) fast in dimension $d = 1$ (or $d > 1$).

This algorithm consists of offline part and online part. In offline part, a set of gPC bases $\{A_i(\omega)\}$ are obtained based on K-L expansion. In online part, the set of gPC bases are used to solve a set of coupled deterministic PDEs of coefficients in the stochastic expansion. It should be noticed that in this framework the set of gPC bases are problem-dependent.

3.1 Offline computation

The purpose of offline computation is to obtain a complete set of gPC bases based on K-L expansion of the stochastic solutions. Instead of using Monte Carlo (MC) simulation, which only has a convergence rate of $1/\sqrt{N}$, we combine sparse grid method and K-L expansion in order to expedite the computation in high dimensional problem. In this part, we obtain not only the gPC bases numerically, but also a variety of statistical information on this set of bases $\{A_i(\omega)\}$, such as expectation of $a(\mathbf{x}, \omega) A_i(\omega) A_j(\omega)$ and moments

$$\mathbb{E}[A_i A_j A_k] = \frac{1}{N} \sum_{n=1}^{N} A_i(\omega_n) A_j(\omega_n) A_k(\omega_n).$$

In order to construct the covariance function $C(\mathbf{x}, \mathbf{y})$, we need to sample stochastic solution $u(\mathbf{x}, \omega)$. First, we expand $u(\mathbf{x}, \omega)$ using polynomial chaos expansion:

$$u(\mathbf{x}, \omega) = \sum \hat{u}_j(\mathbf{x}) \psi_j(\omega). \tag{11}$$

Then by orthogonality of $\{\psi_j(\omega)\}$, we have

$$\hat{u}_j(\mathbf{x}) = \int_{\Omega} u(\mathbf{x}, \omega) \psi_j(\omega) d\omega. \tag{12}$$

The integral (12) can be approximated by sparse grid method,

$$\hat{u}_j(\mathbf{x}) = \sum_i w_i \tilde{u}_i(\mathbf{x}, \omega_i) \psi_j(\omega_i), \tag{13}$$

where $\{\omega_i\}$ are Smolyak sparse grid points, $\{\tilde{u}_i(\mathbf{x},\omega_i)\}$ are corresponding solutions, and $\{w_i\}$ are integration weights associated with $\{\omega_i\}$. Once $\{\hat{u}_j(\mathbf{x})\}$ are obtained, we can sample N solutions $u(\mathbf{x},\omega)$ using K-L expansion (11). Then the mean and covariance are computed

$$\bar{u}(\mathbf{x}) = \frac{1}{N}\sum_{i=1}^{N} u(\mathbf{x},\omega_i), \tag{14}$$

$$C(\mathbf{x},\mathbf{y}) = \frac{1}{N}\sum_{i=1}^{N} u(\mathbf{x},\omega_i)u(\mathbf{y},\omega_i) - \bar{u}(\mathbf{x})\bar{u}(\mathbf{y}). \tag{15}$$

Afterward, the first M eigen-pairs are solved

$$\lambda_i\phi_i(\mathbf{x}) = \int_D C(\mathbf{x},\mathbf{y})\phi_i(\mathbf{y})d\mathbf{y}, \quad i = 1,\cdots,M. \tag{16}$$

Finally, the gPC bases $\{A_i(\omega)\}$ are obtained by

$$A_i(\omega) = \frac{1}{\sqrt{\lambda_i}}\int_D \left(u(\mathbf{x},\omega) - \bar{u}(\mathbf{x})\right)\phi_i(\mathbf{x})d\mathbf{x}. \tag{17}$$

Remark 1 *It is easy to verify that each basis $A_i(\omega)$ has mean zero and $\{A_i(\omega)\}_{i=0}^{M}$ are mutually orthogonal.*

3.2 Online computation

In this part, we only solve deterministic equations since all the statistical information has been obtained in the offline part. This means that the online computation could be fast. The bases $A_i(\omega)$ spans a finite-dimensional subspace in $L^2(\Omega)$. Therefore, we can project the stochastic solution $u(\mathbf{x},\omega)$ onto this subspace, i.e.

$$u(\mathbf{x},\omega) \approx \sum_{i=0}^{M} u_i(\mathbf{x})A_i(\omega). \tag{18}$$

For simplicity of notation, $A_0 = 1$ and $u_0(\mathbf{x}) = \mathbb{E}[u(\mathbf{x},\omega)]$.

In order to obtain the coupled deterministic equations, Galerkin projection is utilized. Multiplying (5) by $A_j(\omega)$ and taking expectation on both sides give us

$$\sum_{i=0}^{M} \mathbb{E}\left[\mathcal{L}(\mathbf{x},\omega)A_i(\omega)A_j(\omega)\right] u_i(\mathbf{x}) = \mathbb{E}\left[f(\mathbf{x})A_j(\omega)\right], \quad j = 0,\cdots,M. \tag{19}$$

4 ANOVA Expansion

In statistics, ANOVA method can be used to describe the interactions between a large number of variables while only few samples are available. The same idea can be adopted in the interpolation and integration of high dimensional problems as well as

stochastic systems. For most well-defined physical system, only relatively low order correlations of the input variables are expected to be important for the output of the system. The ANOVA expansion utilizes this property and at each new level of ANOVA expansion, higher order correlation effects of the input variables are accounted for. Consider a Lebesgue integrable multivariate stochastic function $f(\mathbf{Y}) : \mathbb{R}^d \to \mathbb{R}$ and d is the dimension of stochastic space we are interested in. ANOVA expansion represents $f(\mathbf{Y})$ as finite hierarchical correlated functions of input variables in the form of

$$f(\mathbf{Y}) = f_0 + \sum_{s=1}^{d} \sum_{j_1<\cdots<j_s} f_{j_1,\cdots,j_s}(Y_{j_1}, \cdots, Y_{j_s}), \tag{20}$$

or equivalently

$$\begin{aligned} f(\mathbf{Y}) = f_0 &+ \sum_{1\le j_1\le d} f_{j_1}(Y_{j_1}) + \sum_{1\le j_1<j_2\le d} f_{j_1,j_2}(Y_{j_1}, Y_{j_2}) + \cdots \\ &+ f_{1,2,\cdots,d}(Y_1, Y_2, \cdots, Y_d). \end{aligned} \tag{21}$$

We call $f_{j_k}(Y_{j_k})$ the first order term, $f_{j_k,j_l}(Y_{j_k}, Y_{j_l})$ the second order term, etc. .

The ANOVA components have the following properties:

1. The constant term is the mean of function, that is

$$f_0 = \int_{\Gamma^d} f(\mathbf{Y}) d\mu(\mathbf{Y}), \tag{22}$$

which means that all higher order components have mean zero

$$\int_{\Gamma^d} f_{j_1,\cdots,j_s} d\mu(\mathbf{Y}) = 0 \quad \text{for } 1 \le s \le d. \tag{23}$$

2. The other important property of ANOVA expansion is the orthogonality among its terms

$$\int_{\Gamma^d} f_{j_1,\cdots,j_s} f_{k_1,\cdots,k_l} d\mu(\mathbf{Y}) = 0, \tag{24}$$

if $(j_1, \cdots, j_s) \neq (k_1, \cdots, k_l)$. This is the direct consequence of (23).

3. The variance of f is the sum of variance of all component functions

$$\sigma^2(f) = \sum_{s=1}^{d} \sum_{|\mathbf{s}|=s} \sigma^2(f_{\mathbf{s}}) \tag{25}$$

It is worth pointing out that equation (25) holds only when the measure used in the calculation of variance, i.e. the integral with Lebesgue measure, is the same as that in ANOVA decomposition.

Remark 2 *It could be extremely expensive to compute ANOVA decomposition for high dimensional $f(\mathbf{Y})$. Therefore Dirac measure is adopted instead of Lebesgue measure, i.e. $d\mu(\mathbf{Y}) = \delta(\mathbf{Y} - \mathbf{c})d\mathbf{Y}$, $\mathbf{c} \in \Gamma^d$. The special point $\mathbf{c}$ is termed anchor point. However, it is difficult to calculate anchor point $\mathbf{c}$ such that $f_0 = f(\mathbf{c}) = \overline{f(\mathbf{Y})}$. In this paper, we take anchor point $\mathbf{c}$ to be the mean of random variable $\mathbf{Y}$ as an approximation. In this case, the property* (22) *and* (23) *do not hold any more. Additional terms of ANOVA decomposition are needed to improve the mean.*

The measure $d\mu(\mathbf{Y})$ determines the particular form of each component function following the notation in [29, 28]. We introduce a projection operator $\mathcal{P}_{\mathbf{s}} : \Gamma^d \to \Gamma^{|\mathbf{s}|}$

$$\mathcal{P}_{\mathbf{s}} f(\mathbf{Y}_{\mathbf{s}}) := \int_{\Gamma^{d-|\mathbf{s}|}} f(\mathbf{Y}) d\mu_{I\setminus\mathbf{s}}(\mathbf{Y}) \tag{26}$$

where $d\mu_{I\setminus\mathbf{s}} := \prod_{i\in I, i\notin\mathbf{s}} d\mu_i(Y_i)$.

Therefore, each term $f_{\mathbf{s}}$ can be recursively defined by

$$f_{\mathbf{s}}(\mathbf{Y}_{\mathbf{s}}) = \mathcal{P}_{\mathbf{s}} f(\mathbf{Y}_{\mathbf{s}}) - \sum_{\mathbf{t}\subset\mathbf{s}} f_{\mathbf{t}}(\mathbf{Y}_{\mathbf{t}}). \tag{27}$$

4.1 Adaptive ANOVA

When the nominal dimension of the stochastic problem increases, the computational complexity of the standard ANOVA becomes prohibitive to evaluate all the terms. For example, for nominal dimension $N = 100$, the number of terms for 2nd order ANOVA decomposition needed to calculate is $1 + \binom{100}{1} + \binom{100}{2} = 5051$. Nevertheless, in many stochastic problems, most of the interactions among different dimensions are usually weak and have little contribution to the stochastic outputs. This means that the active dimension of those stochastic problems is small. Therefore, an adaptive approach can be employ to solve those problems efficiently without losing much accuracy.

There are many "adaptive" approaches and the one we employ in this paper is obtained by replacing the nominal dimension by an active dimension, i.e., we modify (21) to be

$$\begin{aligned} f(\mathbf{Y}) \approx f_0 + \sum_{j_1\le D_1} f_{j_1}(Y_{j_1}) + \sum_{(j_1,j_2)\in\mathcal{F}_2} f_{j_1,j_2}(Y_{j_1}, Y_{j_2}) + \cdots \\ + \sum_{(j_1,j_2,,j_\nu)\in\mathcal{F}_\nu} f_{j_1,j_2,\cdots,j_\nu}(Y_{j_1}, Y_{j_2}, \cdots Y_{j_\nu}). \end{aligned} \tag{28}$$

In practice, D_1 is usually set to be N and $\nu = 2$. That is all first order terms are calculated so that some criterion could determine the set $\mathcal{F}_2$ according to the property of the specific problem. However, the criteria in [25, 39] does not specify how many the active dimensions there are a priori. Hence there may be redundant dimensions which are actually not active dimensions. Motivated by the DDSM method, the fast decay of eigenvalues in (7) can serve as an appropriate indicator of the convergence of K-L expansion in terms of optimal gPC bases.

First, we describe two popular adaptive criterion listed in [25, 39]. Then a new criterion is proposed in criterion 3.

Criteria 1: Let $T_1 = \sum_{j=1}^{N} \sigma^2(f_j)$, which is the sum of the variance of all the first-order terms. Assume that the first order terms are sorted such that $\sigma^2(f_j)$ is monotonically decreasing. The active dimension D_2 should satisfy:

$$\sum_{j=1}^{D_2} \sigma^2(f_j) \geq pT_1. \tag{29}$$

where p is a proportionality constant with $0 < p < 1$ and very close to 1. This criterion is similar to the criterion used in [3] where $\sigma^2(f)$ instead of T_1 is used on the right hand side of (29) and p is set to be 0.99. The set $\mathcal{F}$ can be found by computing

$$\eta_{j_1,j_2} = \frac{\sigma^2(f_{j_1,j_2})}{\sum_{j=1}^{D_1} \sigma^2(f_j)}, \tag{30}$$

and bounding η_{j_1,j_2} with a predefined error threshold θ_2.

Criteria 2: Ma and Zabaras use the mean of component function f_j as the indicator to decide the active ANOVA terms [25]. Let

$$\eta_j = \frac{\mathbb{E}(f_j)}{f_0}, \tag{31}$$

where the predefined error threshold θ_1 is used to bound η_j, i.e., $\eta_J \leq \theta_1$ for some J. If η_j are monotonically decreasing with respect to j and we set $D_2 \geq J$, then (31) can equivalently be written as

$$\sum_{j=1}^{D_2} \mathbb{E}(f_j) \geq p \sum_{j=1}^{N} \mathbb{E}(f_j), \tag{32}$$

where $p = 1 - \theta_1$. Then, for a further selection of the second-order terms, Ma and Zabaras also use the mean of the component functions:

$$\eta_{j_1,j_2} = \frac{\mathbb{E}(f_{j_1,j_2})}{\sum_{j=0}^{D_1} E(f_j)}, \tag{33}$$

where η_{j_1,j_2} is bounded by a predefined error threshold θ_2.

Criteria 3: Combining all above, we propose a new criterion, which truly selects active dimensions. First, eigenvalues λ_i of covariance kernel $C(\mathbf{x}, \mathbf{y})$ in equation (7) are obtained and sorted, i.e. $\lambda_1 > \lambda_2 > \cdots$. Then we pick the number of active dimensions D_2 such that

$$\lambda_i/\lambda_1 > \Lambda,\ i = 1, \cdots, D_2, \tag{34}$$

where Λ is a predefined threshold. The dimensions with largest D_2 either variance or mean are selected as active dimensions. Further selection of the second dimensions $\mathcal{F}_2$ could be accomplished by (30) or (33) accordingly. Our numerical examples of 1d and 2d Elliptic PDE with random coefficients show that this criterion is much more efficient by the fact that D_2 is much less than that in Criteria 1 or 2.

Remark 3 *When we employ the above criteria to applications we replace the mean and deviation of component function f_j with their L_2 norm values on the physical domain.*

5 (Adaptive) ANOVA-based Data-Driven Stochastic Method (ANOVA-DDSM)

In this paper, we solve high dimensional stochastic problems by taking advantage of (adaptive) ANOVA method and data-driven stochastic method. For large dimension $d \gg 1$, the rate of convergence in many stochastic methods, such as Monte Carlo method, Wiener Chaos Expansion method (WCE), etc. , deteriorates drastically. This poses a numerical challenge because it requires a huge number of simulations of the underlying deterministic system. This is the well-known curse of dimensionality. The data driven stochastic method also has this problem since the number of gPC bases M increases fast if the dimension of the stochastic problem is large. The following algorithm is proposed to deal with high dimensional stochastic problems efficiently.

Algorithm 1 ((Adaptive) ANOVA-DDSM algorithm)

1. Expand stochastic solution $u(\mathbf{x}, \mathbf{Y})$ in ANOVA decomposition

$$u(\mathbf{x}, \mathbf{Y}) = \quad u_0(\mathbf{x}) + \sum_{j_1=1}^{d} u_{j_1}(\mathbf{x}, Y_{j_1}) + \sum_{1 \le j_1 < j_2 \le d} u_{j_1,j_2}(\mathbf{x}, Y_{j_1}, Y_{j_2}) + \cdots, \tag{35}$$

   or adaptive ANOVA decomposition

$$u(\mathbf{x}, \mathbf{Y}) \approx \quad u_0(\mathbf{x}) + \sum_{j_1=1}^{D_1} u_{j_1}(\mathbf{x}, Y_{j_1}) + \sum_{(j_1,j_2) \in \mathcal{F}_2} u_{j_1,j_2}(\mathbf{x}, Y_{j_1}, Y_{j_2}) + \cdots, \tag{36}$$

   where the set $\mathcal{F}_2$ is selected according to Criterion 3.

2. Solve for the mean term $u_0(\mathbf{x})$ which satisfies a deterministic equation by replacing random variables $\mathbf{Y}$ with anchor point $\mathbf{c}$ in the stochastic PDE,

$$\mathcal{L}(\mathbf{x}, \mathbf{c}) u_0(\mathbf{x}) = f(x). \tag{37}$$

3. For each high order term $u_{j_1,j_2,\cdots,j_s}(Y_{j_1}, Y_{j_2}, \cdots, Y_{j_s})$, DDSM is utilized to calculate the solution efficiently with different deterministic forcing term $f(x)$. For different $f(x)$, the same gPC bases, which have been constructed in the offline part for each term in ANOVA decomposition, can be used repeatedly.

Remark 4 *In practice, only second order or third order terms are needed in (adaptive) ANOVA expansion for good accuracy of mean and variance.*

Remark 5 *In calculating each term in ANOVA expansion, several gPC bases could be enough for accuracy requirement. This essentially expedites our computation.*

6 Numerical examples

As explained in previous sections, we can reduce a high dimensional stochastic problem into a system of low dimensional problems using (adaptive) ANOVA decomposition. For each low dimensional problem, it is significantly efficient to solve each low dimensional problem in terms of CPU time and memory cost.

6.1 1D Stochastic Elliptic PDE in 4d Random Space

We test the ANOVA-DDSM algorithm on a 1D stochastic Elliptic PDE with 4 sources of randomness as follows

$$-\frac{\partial}{\partial x}\left(a(x,\omega)\frac{\partial}{\partial x}u(x,\omega)\right) = f(x), \qquad (38)$$
$$u(x,\omega) = 0, \quad x = 0 \text{ and } x = 1.$$

The stochastic coefficient $a(x,\omega$ in Eq. (38) is chosen to be

$$a(x,\omega) = 1 + \sum_{i=1}^{4} C_i \xi_i(\omega)(\sin(D_i \pi x) + 1), \qquad (39)$$

where

$$C = [0.1,\ 0.12,\ 0.2,\ 0.15], \quad D = [1.2,\ 2.3,\ 3.1,\ 4.3], \qquad (40)$$

and $\{\xi_i\}$ are uniform i.i.d. random variables in $[0,1]$. We run 10^7 realizations of Monte Carlo as the exact solution $u_{MC}(\mathbf{x},\omega)$. The DDSM gPC bases $\{A_i(\omega)\}_{i=1}^{M}$ are constructed using $f(x,y) = 1$ and then are used to solve the stochastic Elliptic PDE with $f(x,y) = \sin(2\pi x) + 5\sin(4\pi y)$. The relative L_2 error of mean is defined as

$$\epsilon_m = \frac{||\bar{u}(\mathbf{x}) - \bar{u}_{MC}(\mathbf{x})||_{L2}}{||\bar{u}_{MC}(\mathbf{x})||_{L2}}, \qquad (41)$$

and relative L_2 error of variance is

$$\epsilon_v = \frac{||\mathrm{Var}\,(u) - \mathrm{Var}\,(u_{MC})||_{L2}}{||\mathrm{Var}\,(u_{MC})||_{L2}}. \qquad (42)$$

The relative error of mean is shown in Fig. 1. The constant term does not represent the mean of the stochastic solution well since the anchor point $\mathbf{c}$ is not optimal. Therefore, additional terms are necessitated to improve the accuracy of ANOVA approach. Note that the stochastic coefficient $a(\mathbf{x},\omega)$ is an additive function of random variables $\xi_i(\omega)$. Then the first order expansion is enough to represent the solution and its mean [25], which is shown in Fig. 1. This plot indicates that increasing the expansion order does not improve accuracy dramatically. Moreover, it only has limited effect on the accuracy of mean by including more gPC bases (or modes) in expansion (18). First order ANOVA expansion and 4 or 5 stochastic modes are good enough to approximate the mean of solution. However, higher order ANOVA decomposition and

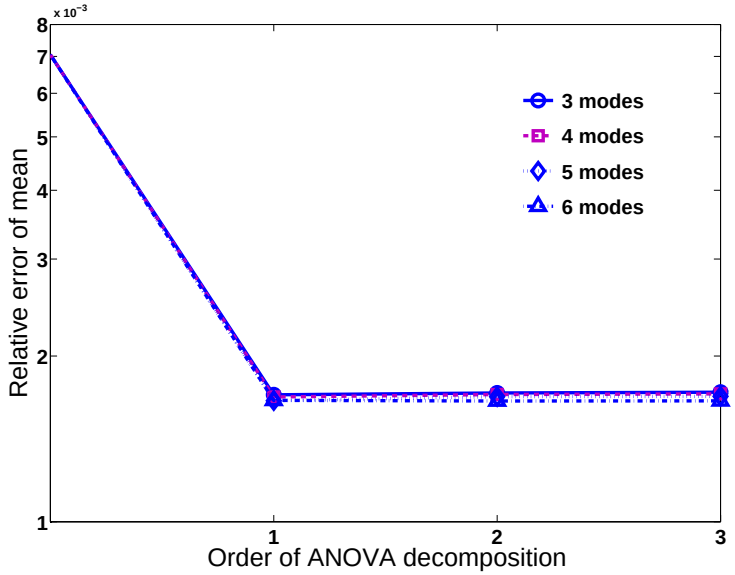

Figure 1: Relative error of mean of one dimensional elliptic PDE with 4 random variables. The exact solution is computed with 10^7 realizations.

more stochastic modes are required to represent the variance well. As shown in Fig. 2, second order of ANOVA decomposition and 6 bases are needed to approximate the variance of stochastic solution. Contrast to the mean, increasing the order of ANOVA decomposition and/or number of stochastic bases do improve the accuracy of variance. In practice, unless otherwise stated, we take second order ANOVA expansion and 6 gPC bases in our calculations.

6.2 1D Stochastic Elliptic PDE in High Dimensional Probabilistic Space

In this subsection, we consider 1D stochastic Elliptic PDE (38) in 100 dimensional probabilistic space. The stochastic coefficient $a(x,\omega)$ now reads as

$$a(x,\omega) = \sum_{i=1}^{100} C_i \xi_i(\omega)(\sin(D_i \pi x) + 1), \tag{43}$$

where $\{\xi_i\}$ are uniform random variables in $[0,1]$ and $C_i \in (0, 0.001)$ and $D_i \in (0, 10)$ are randomly generated. We run 10^6 realizations of Monte Carlo as the reference solution $u_{MC}(\mathbf{x},\omega)$. The DDSM gPC bases $\{A_i(\omega)\}_{i=1}^M$ are constructed using $f(x,y) = 1$ and then are used to solve the stochastic Elliptic PDE with $f(x,y) = \sin(2\pi x) + 5\sin(4\pi y)$.

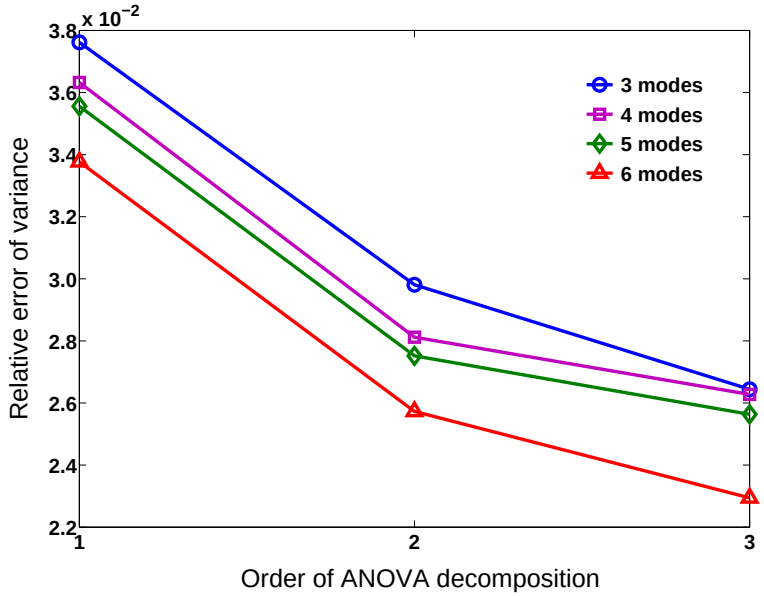

Figure 2: Relative error of variance of one dimensional elliptic PDE with 4 random variables. The exact solution is computed with 10^7 realizations.

Table 1: Comparison of adaptive ANOVA-DDSM using different Criteria

	relative error of mean		relative error of σ		# of active terms	
Criterion 1 (p = 0.9, η_{j_1,j_2}=1E-5)	2.04E-2		2.14E-2		151	
Criterion 3	Λ = 1E-3	Λ = 1E-5	Λ =1E-3	Λ =1E-5	Λ =1E-3	Λ =1E-5
	3.60E-2	2.23E-2	2.21E-2	2.15E-2	111	146

The decay of λ_i/λ_1 is shown in Figure 3. Only 5 dimensions are active if Λ =1E-3 and 10 dimensions if Λ =1E-5. However, if we pick $p = 0.9$, the numbers of active dimensions are 54 and 87 for Criterion 1 and 2 respectively. Thus, the numbers of second order terms needed to be computed are 1431 and 3741 respectively. The computations of all these terms are necessary, although the number of active terms in second order could be further shrinked by imposing some threshold η_{j_1,j_2} for the relative variance or mean in Criterion 1 or 2. In contrast, in Criterion 3, the active dimensions have been identified beforehand for some predefined threshold Λ. Thus the number of second order terms needed to compute is significant less.

The comparison using Criteria 1 and 3 is listed in Table 1. From this table, it is clear that, using different criteria, the numbers of final active terms are almost the same and so are the relative errors of mean and standard deviation σ.

The profile of mean computed by second order adaptive ANOVA-DDSM using Criterion 3 is compared with MC method in Fig. 4. It can be seen that the profile

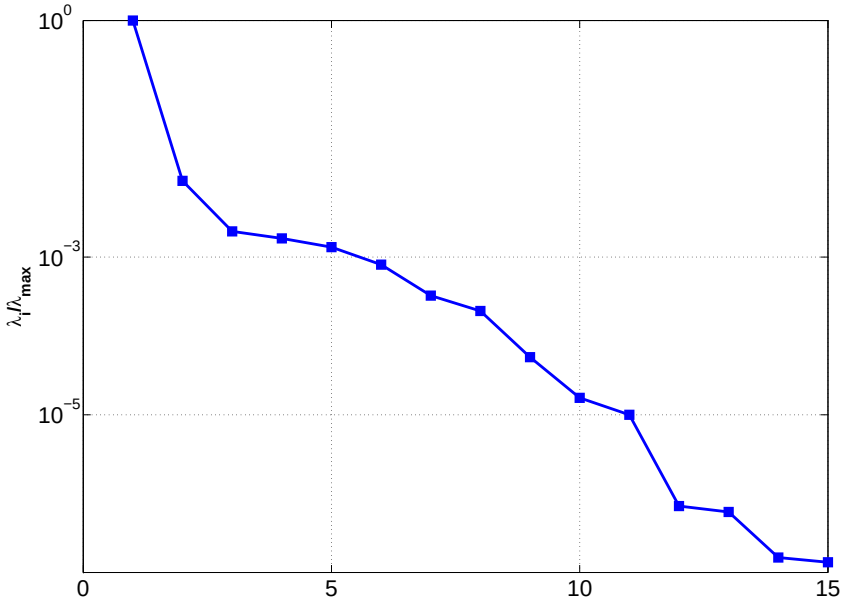

Figure 3: The decay of sorted relative eigenvalues of covariance kernel for a 1D Elliptic PDE with random coefficient in 100 probabilistic dimension.

matches the reference solution very well. However, the standard deviation of ANOVA-DDSM is a little lower than MC as shown in Fig. 5. Higher order adaptive ANOVA decomposition can definitely improve the accuracy of standard deviation. But it brings considerably more amount of computations.

6.3 Horn Problem

In this subsection, we extend our method to 2-d Helmholtz equation in random media, the planar acoustics horn problem described in detail in [34]. The full domain is depicted in Fig. 6, which comprises both the horn proper and a large circular segment. The governing equations for the (complex) pressure are then

$$\nabla^2 p(x,y,\omega) + k^2(1+n^2(x,y,\omega))p(x,y,\omega) = 0, \tag{44}$$

with boundary conditions

$$\begin{aligned} \frac{\partial p}{\partial \vec{n}} - ikp &= 0 \quad \text{on } \Gamma_1, \\ \frac{\partial p}{\partial \vec{n}} &= 0 \quad \text{on } \Gamma_2, \\ p(x,y,\omega) &= f(x,y) \quad \text{on } \Gamma_3, \end{aligned}$$

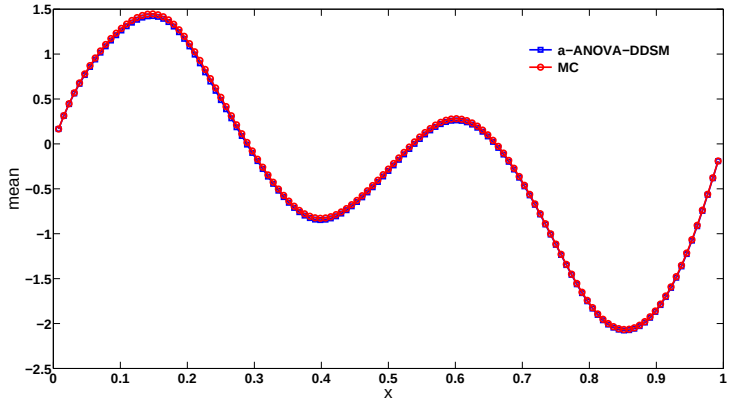

Figure 4: Comparison of mean of one dimensional elliptic PDE with 100 random variables by Adaptive ANOVA-DDSM using Criterion 3 and Monte Carlo simulation. Λ =1E-5 and 10 active dimensions.

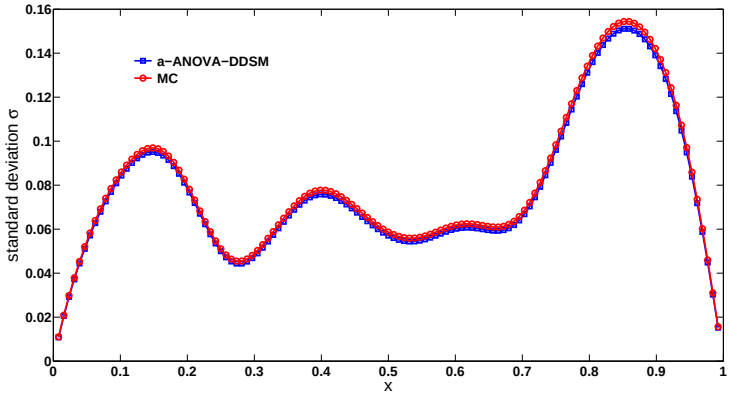

Figure 5: Comparison of standard deviation of one dimensional elliptic PDE with 100 random variables by Adaptive ANOVA-DDSM using Criterion 3 and Monte Carlo simulation. Λ =1E-5 and 10 active dimensions.

where $\vec{n}$ is the unit outer-pointing normal of the boundary, k is the wave number and $n^2(x, y, \omega)$ is the random reflectivity of the media. In this example, the random reflectivity of the media is chosen to be

$$n^2(x, y, \omega) = \sum_{i=1}^{4} \xi_i(\omega)\psi_i(x, y),$$

where $\{\xi_i(\omega)\}$ are i.i.d. uniformly distributed random variable in $[0, 1]$ and functions $\{\psi_i(x, y)\}$ are given by

$$\begin{aligned}
\psi_1(x, y) &= \sin^2(2\pi x + \theta_1)\sin^2(2\pi y + \theta_2) \\
\psi_2(x, y) &= \sin^2(4\pi x + \theta_3)\sin^2(4\pi y + \theta_4) \\
\psi_3(x, y) &= \sin^2(6\pi x + \theta_5)\sin^2(4\pi y + \theta_6) \\
\psi_4(x, y) &= \sin^2(6\pi x + \theta_7)\sin^2(6\pi y + \theta_8)
\end{aligned}$$

with phase $\{\theta_i\}$ being randomly generated.

The DDSM gPC bases $\{A_i(\omega)\}_{i=1}^{M}$ are constructed using $f(x, y) = 1$ and then are used to solve the stochastic horn problem with $f(x, y) = \sin(2\pi x)\sin(2\pi y) + 2$. In this example, k is taken to be 0.7. Only 6 gPC bases and second order ANOVA decomposition are used. In Fig. 7, the comparison of real part of mean contours of pressure by ANOVA-DDSM and MC methods is shown. As expected, the mean could be approximated accurately even using only second order ANOVA decomposition in this example. However, the difference of standard deviation is noticeable, especially outside the horn proper and the region right of center. Again, this is mainly due to the lower order of ANOVA decomposition. Accuracy of deviation could be compensated by employing higher order ANOVA decomposition and/or more gPC bases. Adaptive ANOVA method could be utilized if computational cost is highly concerned and high accuracy is required.

6.4 2D Stochastic Elliptic PDE in High Dimensional Probabilistic Space

Finally, We consider a 2D stochastic Elliptic PDE with a random coefficient in 50 dimensional probabilistic space

$$\begin{aligned}
-\nabla \cdot (a(x, y, \omega)\nabla u(x, y, \omega)) &= f(x, y), \\
u(x, y, \omega)|_{\partial D} &= 0.
\end{aligned} \tag{45}$$

The stochastic coefficient $a(x, y, \omega)$ is defined as

$$a(x, y, \omega) = \sum_{i=1}^{50} D_i\xi_i \left(\sin(E_i\pi x + F_i\pi y) + 1\right), \tag{46}$$

where $\{\xi_i\}$ are uniform random variables in $[0, 1]$ and the constant parameters are randomly generated $D_i \in [0, 0.01], E_i, F_i \in [5, 10]$. Adaptive ANOVA-DDSM methods

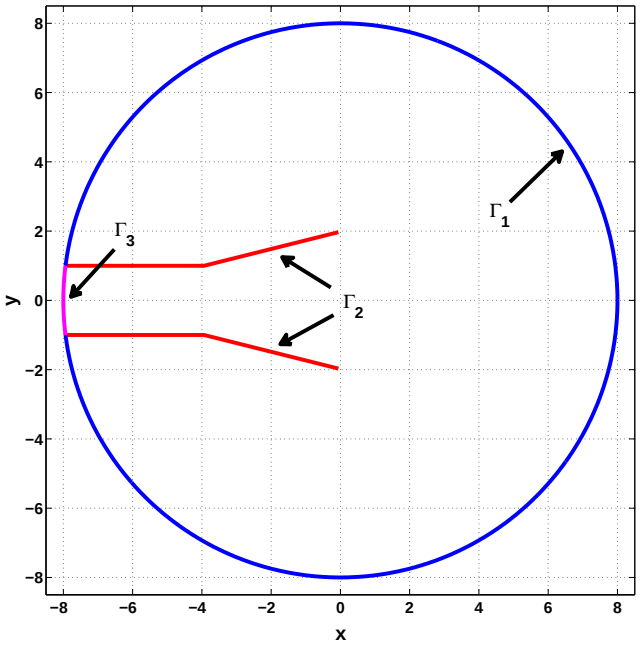

Figure 6: Geometry of horn problem

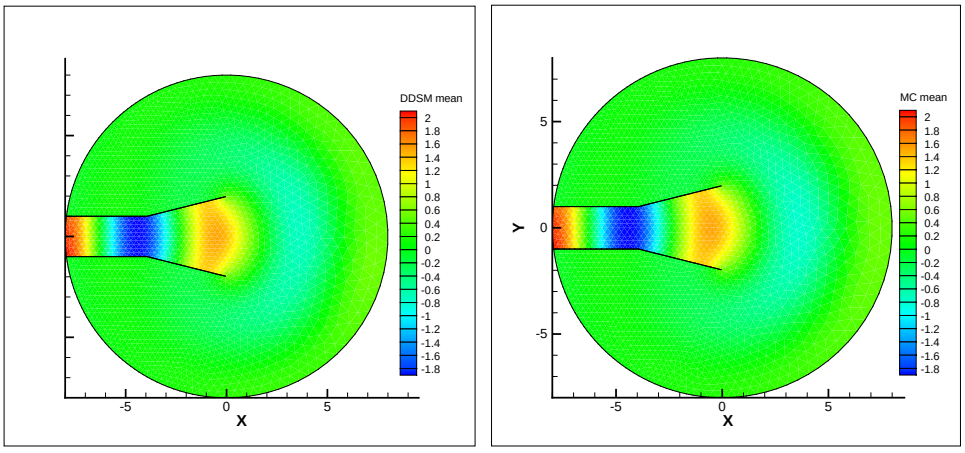

Figure 7: Comparison of real part of mean contour in horn problem. Left: ANOVA-DDSM method. Right: Monte-Carlo simulation.

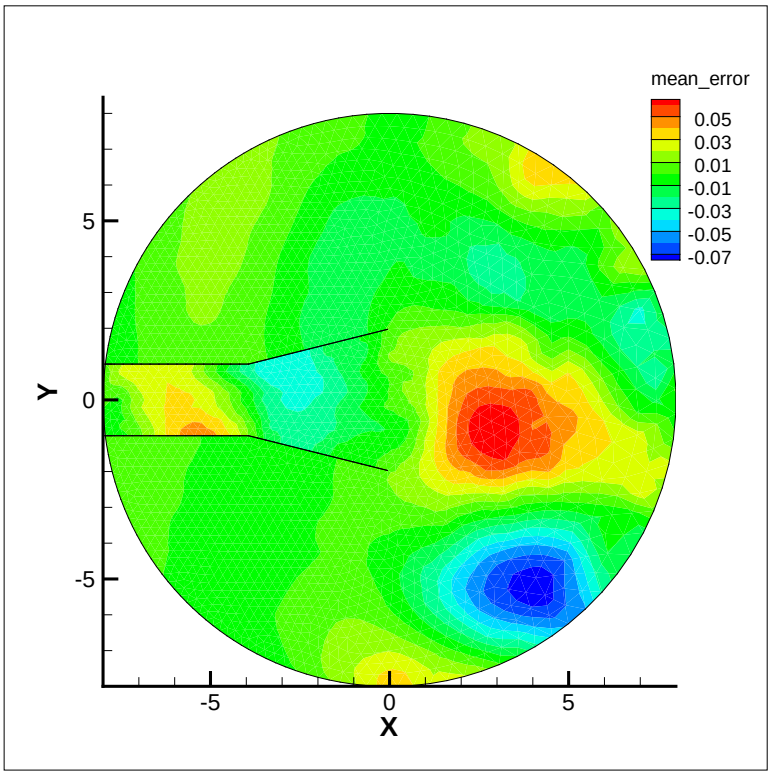

Figure 8: Error of real part of mean contour in horn problem.

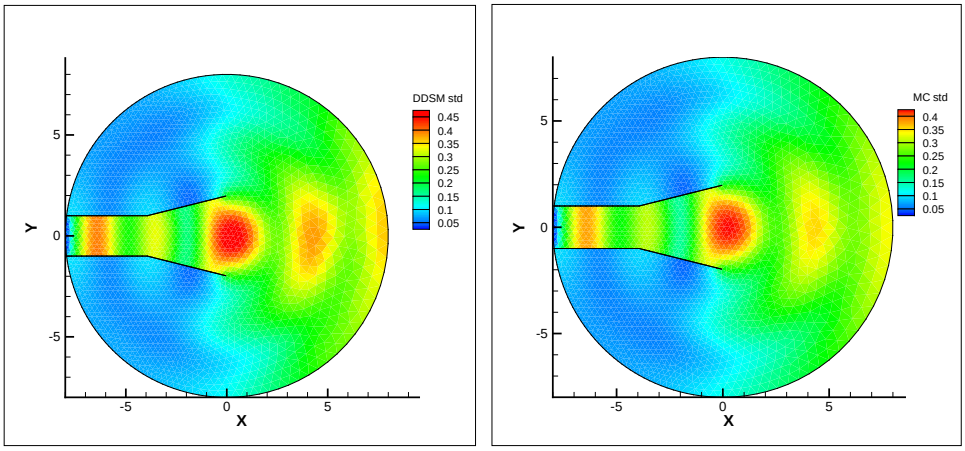

Figure 9: Comparison of standard deviation contour in horn problem. Left: ANOVA-DDSM method . Right: Monte-Carlo simulation.

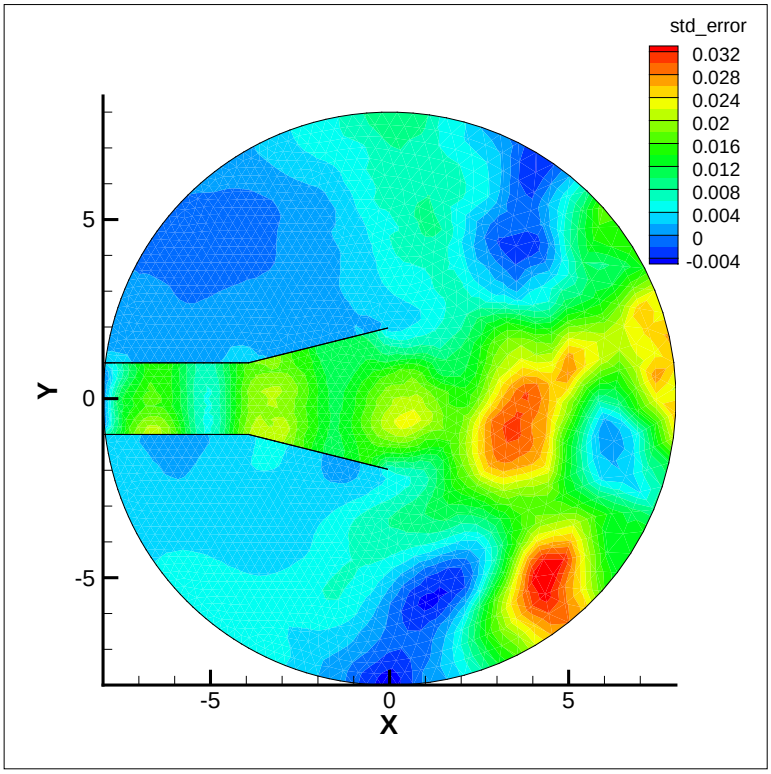

Figure 10: Error of standard deviation contour in horn problem.

Table 2: Comparison of adaptive ANOVA-DDSM using different Criteria

	relative error of mean		relative error of σ		# of active terms	
Criterion 1 (p = 0.99, η_{j_1,j_2}=1E-5)	3.60E-3		5.70E-2		201	
Criterion 3	$\Lambda = $ 1E-3	$\Lambda = $ 1E-4	$\Lambda = $1E-3	$\Lambda = $1E-4	$\Lambda = $1E-3	$\Lambda = $1E-4
	4.60E-3	4.40E-3	6.72E-2	6.18E-2	61	96

using different criteria are employed to solve this problem. The DDSM gPC bases $\{A_i(\omega)\}_{i=1}^M$ are constructed using $f(x,y) = 1$ and then are used to solve the stochastic Elliptic PDE with $f(x,y) = \sin(2\pi x)\sin(2\pi y) + 2$. Monte-Carlo results with 10^6 realizations are served as reference solutions. The decay plot of eigen-values of covariance kernel in Fig. 11 indicates that there are 5 active dimensions if $\lambda_i/\lambda_1 >$1E-3 and 10 active terms if $\lambda_i/\lambda_1 >$1E-4 in Criterion 3. For Criterion 1, the parameter p is set to be 0.99, which results in 25 active dimensions. Then total 300 second order terms are computed. It requires 201 terms in total for $\eta_{(j_1,j_2)} =$1E-5 to be calculated towards approximating stochastic outputs. In contrast, to achieve the same order of accuracy for both mean and standard deviation, there are only 61 and 96 terms needed in total for $\Lambda =$1E-3 and $\Lambda =$1E-4, respectively. The comparison results are summarized in Table 2.

In Fig. 12, the contour of mean computed by adaptive ANOVA-DDSM using Criterion 3 with 10 active dimensions is plotted and compared with that by MC. In terms of mean, adaptive ANOVA-DDSM performs well. To further demonstrate the convergence of mean, we plot the error contour of mean in Fig. 13. This shows clearly that the magnitude of error is of order 10^{-2}. In addition, we plot the mean contour lines of stochastic solutions given by adaptive ANOVA-DDSM and MC in Fig. 14. Again, the contours match very well. All the above have shown that ANOVA-DDSM captures mean accurately.

In Fig. 15, the contour of standard deviation computed by adaptive ANOVA-DDSM using Criterion 3 with 10 active dimensions is plotted and compared with that by MC. Adaptive ANOVA-DDSM can capture the correct pattern of the standard deviation. However, the magnitude is slightly lower. This is indicated in Fig. 16, where the error of standard deviation is plotted. In order to further illustrate this, the contour lines of standard deviation are shown in Fig. 17. The closer to the center of the domain, the larger the solution is. In this plot, the contour lines of adaptive ANOVA-DDSM are closer to the center than those of MC, which means that the deviation calculated by adaptive ANOVA-DDSM is smaller. This is mainly due to the following two facts. First, only 10 active dimensions in adaptive ANOVA decomposition are considered and this is just an approximation of the standard ANOVA decomposition. Secondly and more importantly, only second order decomposition is employed. Using higher order adaptive ANOVA decomposition could improve the accuracy of standard deviation, but it would take much more computational cost.

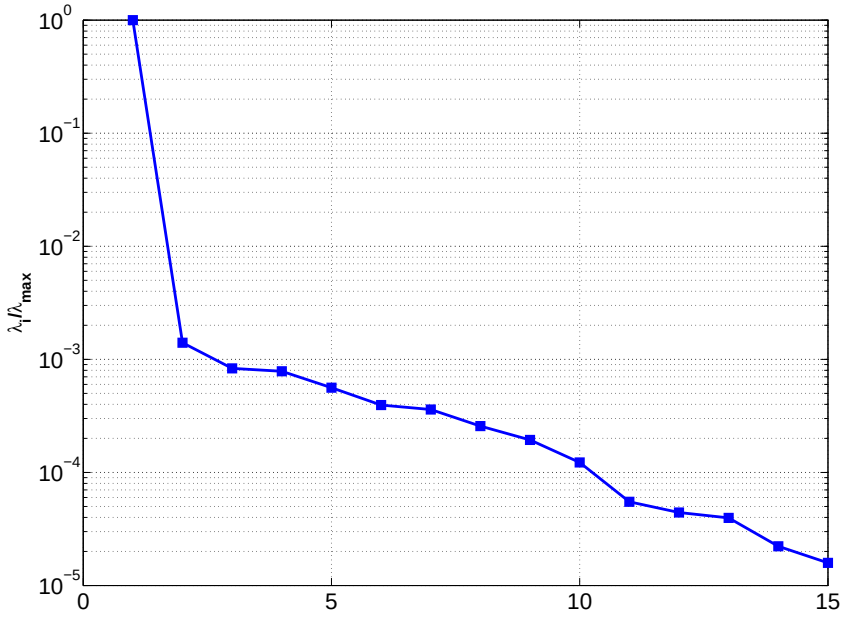

Figure 11: The decay of sorted relative eigenvalues of covariance kernel for a 2D Elliptic PDE with random coefficient in 50 probabilistic dimension.

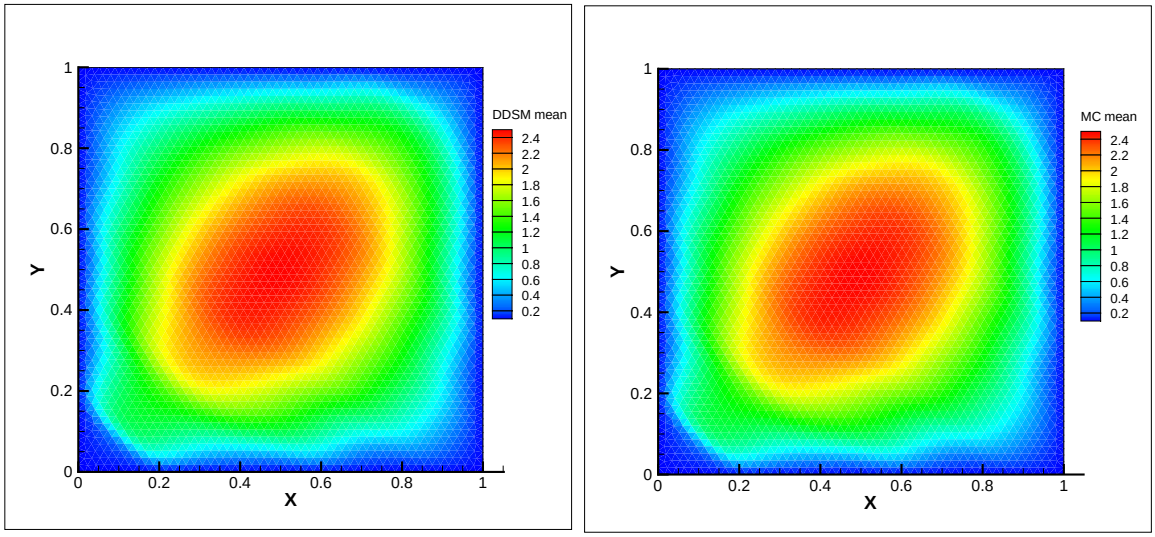

Figure 12: Comparison of mean contour of 2D stochastic Elliptic PDE. Left: adaptive ANOVA-DDSM method using Criterion 3. Right:Monte-Carlo simulation. Λ =1E-4 and 10 active dimensions.

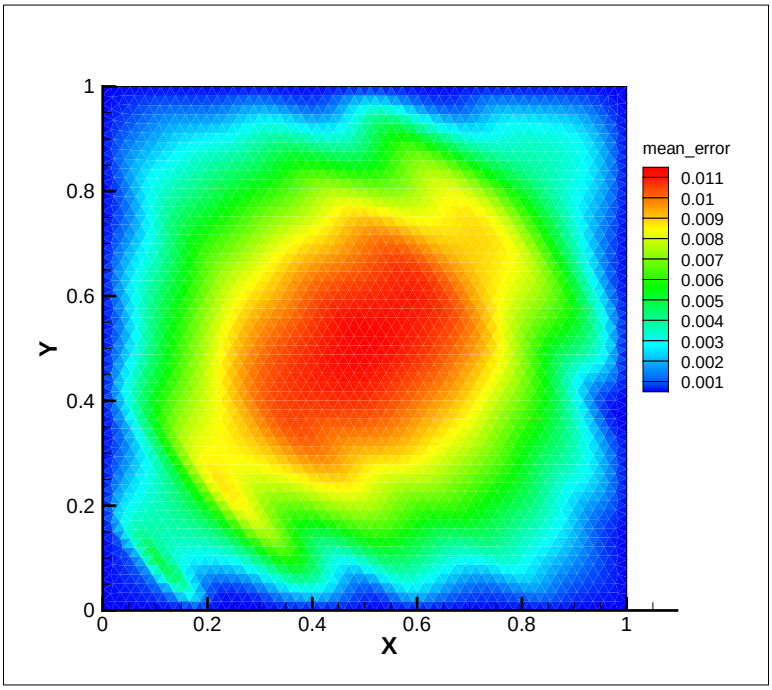

Figure 13: Mean error contour of 2D stochastic Elliptic PDE.

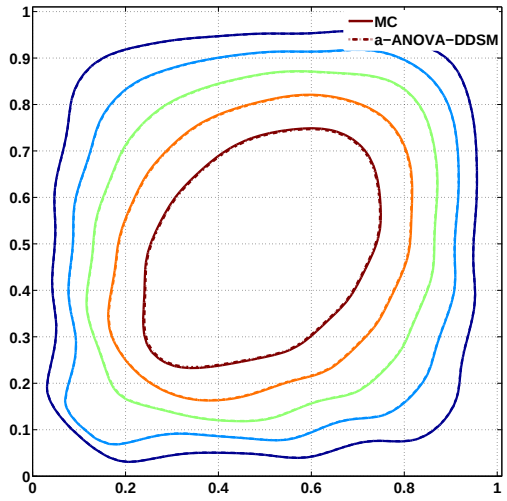

Figure 14: Contour comparison of mean contour of 2D stochastic Elliptic PDE.

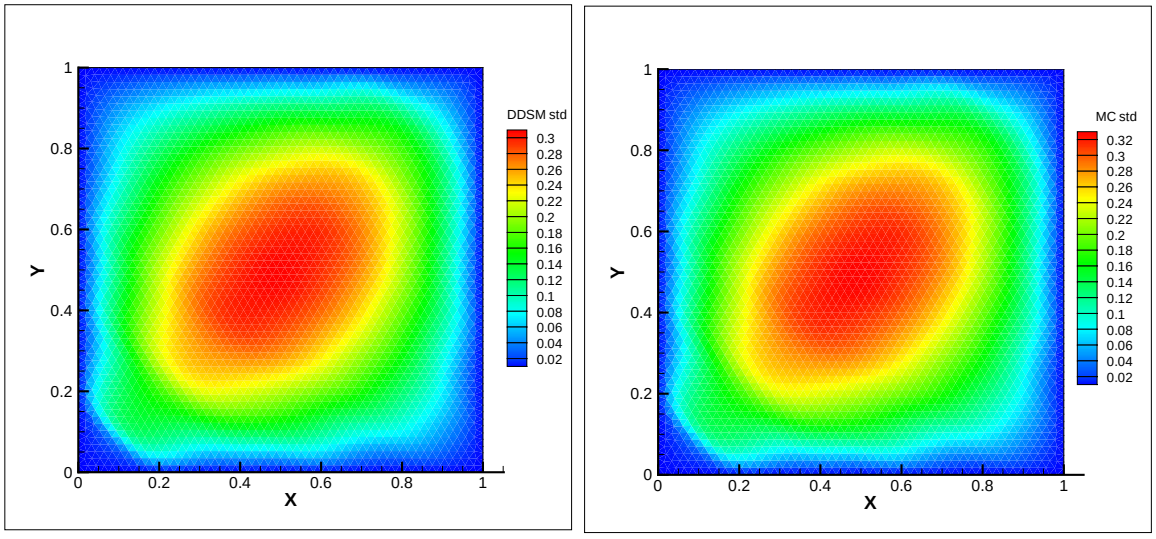

Figure 15: Comparison of standard deviation contour of 2D stochastic Elliptic PDE. Left: adaptive ANOVA-DDSM method using Criterion 3. Right: Monte-Carlo method. Λ =1E-4 and 10 active dimensions.

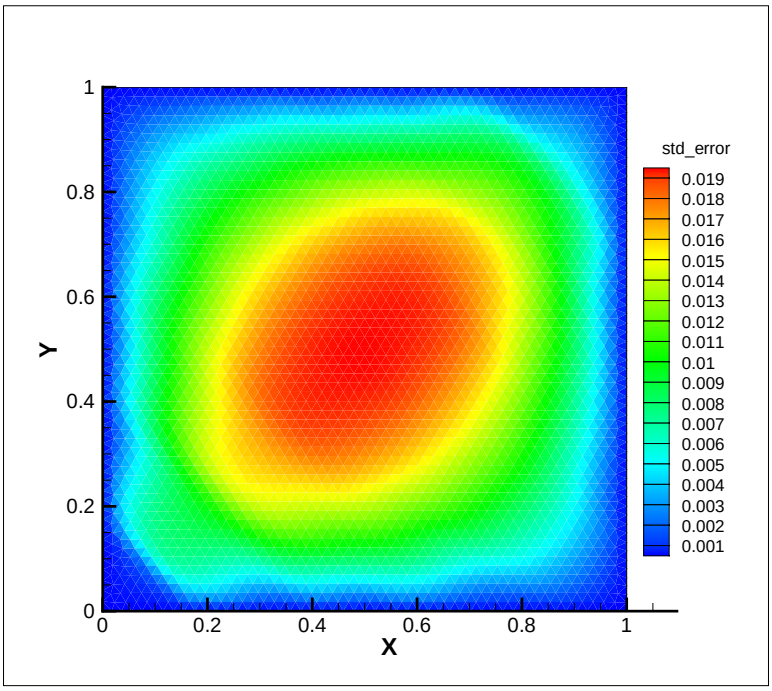

Figure 16: Standard deviation error contour of 2D stochastic Elliptic PDE.

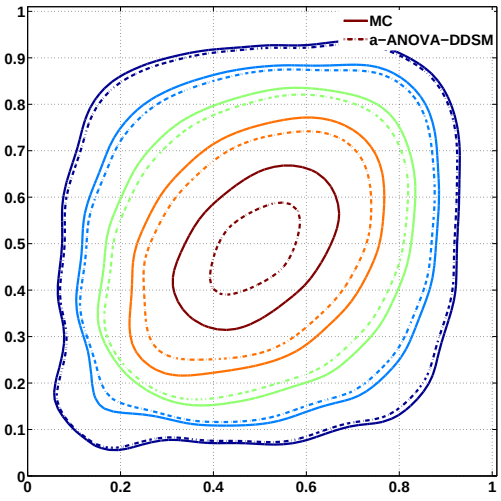

Figure 17: Contour comparison of standard deviation contour of 2D stochastic Elliptic PDE.

7 Conclusion and Discussion

In this paper, a novel adaptive ANOVA-based data-driven method is developed for solving high-dimensional stochastic elliptic equation arising from various applications, such as the randomly heterogeneous porous media flow problem. The developed method has an offline computation and an online computation. In the offline computation, adaptive ANOVA decomposition technique is applied to adaptively decompose the original high dimensional problem into a set of low-dimensional sub-problems. By modeling the behavior of stochastic systems with only the first few lower-order terms of the high-dimensional input, adaptive ANOVA is able to efficiently represent the output response to the high-dimensional inputs with specified good accuracy. This results in a set of low-dimensional sub-problems in stochastic space, which are efficiently solved by sparse-grid PCM. Numerical examples have shown that solving the set of low-dimensional sub-problems is more efficient than solving the original problem. Three different ANOVA adaptive criterion are discussed. Numerical tests indicate that the third adaptive criteria gives the best approximation with minimal computational cost.

Numerical examples involving both one-, two-dimensional elliptic PDE with random coefficients, and a two-dimensional Helmhotz equation in random media (Horn problem) have been conducted to verify the accuracy and efficiency of the developed adaptive ANOVA-based DDSM method. In the offline computation, for stochastic problems with fixed number of stochastic dimension, the number of component functions needed in adaptive ANOVA decomposition depends on the important dimensions with respect to the stochastic outputs and the variance of the stochastic inputs. For real physical high-dimensional stochastic problems with up to $500 - 600$ stochastic dimensions [9, 25], adaptive ANOVA decomposition integrated with sparse-grid PCM can achieve much better convergence rate than both the Monte Carlo and sparse-grid PCM. However, it is worthwhile to note that adaptive ANOVA decomposition may not be recommended to approximate mathematical functions where all dimensions are important. Additionally, sparse-grid PCM is determined based on the probabilistic distribution of stochastic inputs. However, due to the nonlinearity of the complex stochastic systems, the numerical solutions may not share the same probabilistic distribution as the stochastic inputs. Hence, the distribution used for sparse-grid PCM may not be the optimal distribution to represent the solutions of such systems, which causes the slow convergence of sparse-grid PCM for such stochastic problems.

To improve the slow convergence, optimal gPC bases are obtained by the K-L expansion of the covariance matrix of the stochastic output solutions computed by the adaptive ANOVA-based sparse-grid PCM. In the online computation, a Galerkin-projection based gPC method with the optimal bases developed in the offline computational part is employed, which greatly improves the convergence rate. The obtained results in numerical examples considered indicate following three advantages of the proposed adaptive ANOVA-based DDSM method: (1) by integrating with adaptive ANOVA decomposition, it can effectively solve stochastic problems within desire accuracy even for problems with high-dimensional and large variance stochastic inputs; (2) the same optimal bases can be used for various deterministic forcing terms on the right-hand-side function of the elliptic PDE with random coefficients; (3) comparing to

the classic gPC method, the number of gPC modes to achieve specified accuracy used in the adaptive ANOVA-based DDSM method is much smaller, which greatly reduces the computational cost.

Acknowledgement

This work was supported by the U.S. Department of Energy (DOE) Office of Science Advanced Scientific Computing Research Applied Mathematics program. The work of Hou was supported in part by an AFOSR MURI project under Contract FA9550-09-1-0613. A portion of the computations were performed using PNNL Institutional Computing cluster systems and EMSL, a national scientific user facility sponsored by the DOE Office of Biological and Environmental Research and located at Pacific Northwest National Laboratory (PNNL), as well as computational resources from the National Energy Research Scientific Computing Center at Lawrence Berkeley National Laboratory. PNNL is operated by Battelle for the DOE under Contract DE-AC05-76RL01830.

References

[1] V. Barthelmann, E. Novak, and K. Ritter. High dimensional polynomial interpolation on sparse grids. *Adv. Comput. Math.*, 12:273–288, 2000.

[2] M. Bieri and C. Schwab. Sparse high order fem for elliptic spdes. *Comput. Methods Appl. Mech. Engrg.*, 198:1149–1170, 2009.

[3] R.E. Caflisch, W. Morokoff, and A. Owen. Valuation of mortgage-backed securities using brownian bridges to reduce the effective dimension. *J. Comput. Finance*, 1:27–46, 1997.

[4] Y. Cao, Z. Chen, and M. Gunzburger. ANOVA Expansions and Efficient Sampling Methods for Parameter Dependent Nonlinear PDEs. *Int. J. Numer. Analysis and Modeling*, 6(2):256–273, 2009.

[5] M. Cheng, T. Y. Hou, and M. Yan. A data-driven stochastic method. 2011.

[6] R. Cools. Monomial cubature rules since ‘stroud’: A compilation. *J. Comput. Appl. Math.*, 48:309–326, 1993.

[7] R. Cools. Monomial cubature rules since ‘stroud’: A compilation - part 2. *J. Comput. Appl. Math.*, 112:21–27, 1999.

[8] R. Fisher. *Statistical Methods for Research Workers*. Oliver and Boyd, 1925.

[9] Jasmine Y. Foo and George Em Karniadakis. Multi-element probabilistic collocation in high dimensions. *J. Comput. Phys.*, 229:1536–1557, 2009.

[10] B. Ganapathysubramanian and N. Zabaras. Sparse grid collocation schemes for stochastic natural convection problems. *J. Comput. Phys.*, 225(1):652–685, 2007.

[11] Z. Gao and J.S. Hesthaven. On ANOVA Expansions and Stragies for Choosing the Anchor Point. *App. Math. Comp.*, 217(7):3274–3285, 2009.

[12] T. Gerstner and M. Griebel. Dimension-adaptive tensor-product quadrature. *Computing*, 71(1):65–87, 2003.

[13] G.Lin and G.E.Karniadakis. Sensitivity analysis and stochastic simulations of non-equilibrium plasma flow. *Int. J. Numer. Meth. Engng*, 80(6-7):738–766, March 2009.

[14] M. Griebel. Adaptive sparse grid multilevel methods for elliptic pdes based on finite differences. *Computing*, 61(2):151–180, 1998.

[15] M. Griebel. *Sparse grids and related approximation schemes for higher-dimensional problems*. Proceedings of the conference on Foundations of Computational Mathematics, Santander, Spain, 2005.

[16] W. Hoeffding. A class of statistics with asymptotically normal distributions. *Annals of Math. Statist.*, 19:293–325, 1948.

[17] T.Y. Hou and X. Wu. A multiscale finite element method for elliptic problems in composite materials and porous media. *J. Comp. Phys.*, 134(1):169–189, 1997.

[18] G. Lin, C.-H. Su, and G.E. Karniadakis. Predicting shock dynamics in the presence of uncertainties. *J. Comp. Phys.*, 217:260–276, 2006.

[19] G. Lin and A.M. Tartakovsky. An efficient, high-order probabilistic collocation method on sparse grids for three-dimensional flow and solute transport in randomly heterogeneous porous media. *Advances in Water Resources*, 32(5):712–722, 2009.

[20] G. Lin and A.M. Tartakovsky. Numerical studies of three-dimensional stochastic Darcy's equation and stochastic advection-diffusion-dispersion equation. *Journal of Scientific Computing*, 43(1):92–117, 2010.

[21] Guang Lin, Chau-Hsing Su, and George Em Karniadakis. Random roughness enhances lift in supersonic flow. *Physical Review Letters*, 99:104501, 2007.

[22] Guang Lin, Chau-Hsing Su, and George Em Karniadakis. Stochastic modeling of random roughness in shock scattering problems: Theory and simulations. *Comput. Methods Appl. Mech. Engrg.*, 197:3420–3434, 2008.

[23] X. Ma and N. Zabaras. An adaptive hierarchical sparse grid collocation algorithm for the solution of stochastic differential equations. *J. Comput. Phys.*, 228(8):3084–3113, 2009.

[24] Xiang Ma and Nicholas Zabaras. An adaptive hierarchical sparse grid collocation method for the solution of stochastic differential equations. *J. Comput. Phys.*, 228:3084–3113, 2009.

[25] Xiang Ma and Nicholas Zabaras. An adaptive high-dimensional stochastic model representation technique for the solution of stochastic partial differential equations. *J. Comp. Phys.*, 229:3884–3915, 2010.

[26] E. Novak and K. Ritter. High dimensional integration of smooth funcions over cubes. *Numer. Math.*, 75:79–97, 1996.

[27] E. Novak and K. Ritter. Simple cubature formulas with high polynomial exactness. *Constr. Approx.*, 15:499–522, 1999.

[28] H. Rabitz and Ö. F. Aliş. General foundations of high-dimensional model representations. *J. Math. Chem.*, 25:197–233, 1999.

[29] H. Rabitz, Ö. F. Aliş, J. Shorter, and K. Shim. Efficient input-output model rep. *Comput. Phys. Commun.*, 117:11–20, 1999.

[30] Christoph Schwab and Radu Alexandru Todor. Karhunen loève approximation of random fields by generalized fast multipole methods. *J. Comp. Phys.*, 217:100–122, 2006.

[31] L. Sirovich. Turbulence and the dynamics of coherent structures, parts i, ii and iii. *Q. Appl. Maths XLV*, pages 561–590, 1987.

[32] S. Smolyak. Quadrature and interpolation formulas for tensor products of certain classes of functions. *Soviet Math. Dokl.*, 4:240–243, 1963.

[33] M. Tatang and G. McRae. Direct treatment of uncertainty in models of reaction and transport. Technical report, MIT Tech. Rep., 1994.

[34] R. Udawalpola and M. Berggren. Optimization of an acoustic horn with respect to efficiency and directivity. *Int. J. Numer. Mech. Eng*, 73:1571–1606, 2008.

[35] D. Venturi, X. Wan, and G. E. Karniadakis. Stochastic low dimensional modeling of random laminar wake past a circular cylinder. *J. Fluid Mech.*, 606:339–367, 2008.

[36] C.L. Winter, A. Guadagnini, D. Nychka, and D.M. Tartakovsky. Multivariate sensitivity analysis of saturated flow through simulated highly heterogeneous groundwater aquifers. *J. Comput. Phys.*, 217:166–175, 2009.

[37] D. Xiu and J. S. Hesthaven. High order collocation methods for differential equations with random inputs. *SIAM J. Sci. Comput.*, 27(3):1118–1139, 2005.

[38] D. Xiu and G. E. Karniadakis. The Wiener-Askey polynomial chaos for stochastic differential equations. *SIAM J. Sci. Comput.*, 24(2):619–644, 2002.

[39] Xiu Yang, Minseok Choi, Guang Lin, and George Em Karniadakis. Adaptive anova decomposition of stochastic incomressible and comressible flows. *J. Comp. Phys.*, page doi:10.1016/j.jcp.2011.10.028, 2011.